Tutor/s

Dra.Anna de Juan Capdevila
Departament d'Enginyeria Química i Química Analítica

Dra.Carmen Bedia Girbes
CSIC-IDAEA

Grau de Química

Treball Final de Grau

Mass spectometry imaging: optimization of sample preparation and metabolite identification through MS/MS.

Espectrometria de masses d'imatge: optimització de preparacions de mostra i identificació de metabòlits per MS/MS.

Nora Fernández Navas

June 2017

UNIVERSITAT DE BARCELONA

B:KC Barcelona Knowledge Campus
Campus d'Excel·lència Internacional

En la vida no existe nada que temer, solo cosas por comprender.

Marie Curie

Primer de tot, voldria fer una menció especial a la meva tutora Dra.Carmen Bedia per tot el que he après gràcies a ella, la gran dedicació i ajuda en el treball i la paciència que ha tingut durant aquests mesos. També agraïr a la Dra. Anna de Juan pel seu seguiment i resoldre'm els dubtes que han anat sortint durant el treball.

Al meu tutor Dr. Fermín Huarte per donar-me suport durant tota la carrera.

I finalment, als meus amics, família i parella que han hagut d'aguantar el meu mal humor en èpoques d'examens, i les meves indecisions i mil canvis d'idees durant aquests quatre anys.

REPORT

CONTENTS

1. SUMMARY

Metabolomics consists in the study of small molecules called metabolites which are present in living organisms. These low mass compounds are the ultimate answer to perturbations produced in the organism. Therefore, their quantification and identification lead to a reading out of the cellular state. In order to obtain this information, analytical techniques are employed. The use of mass spectrometry imaging allows to obtain structural and spatial distribution information of the studied sample. Two important points are considered when this analysis is undergone: tissue sample preparation and metabolites identification. The present work is focused to improve these difficulties in various plant tissues utilizing Matrix Assisted Laser Desorption Ionization (MALDI) imaging as instrument.

This project has been carried out at the Institut de Diagnosi Ambiental i Estudis de l'Aigua (IDAEA) laboratories of Consell Superior d'Investigacions Científiques (CSIC).

Keywords: Metabolomics, cellular state, mass spectrometry imaging, MALDI, plant tissues.

2. RESUM

La metabolòmica consisteix en l'estudi de molècules de baix pes molecular anomenades metabolits i que es troben presents a tots els organismes. Aquests compostos, són l'última resposta als canvis als quals està sotmès l'organisme. De forma que, la seva quantificació i identificació permet obtenir informació sobre l'estat cel·lular. Per tal d'adquirir aquesta informació s'utilitzen tècniques analítiques. L'ús de l'espectrometria de masses d'imatges proporciona informació sobre l'estructura i la distribució espacial de la mostra estudiada. A l'hora de dur a terme l'anàlisi s'han de considerar dos aspectes fundamentals: la preparació de la mostra i l'identificació dels metabolits. Per aquesta raó, aquest treball es basa en la millora d'aquests "obstacles" en diversos teixits de plantes. La tècnica utitzada és Matrix Assisted Laser Desorption Ionization (MALDI) imaging.

El projecte s'ha dut a terme a les instal·lacions de l'Institut de Diagnosi Ambiental i Estudis de l'aigua (IDAEA) del Consell Superior d'Investigacions Científiques (CSIC).

Paraules clau: Metabolòmica, estat cel·lular, espectrometria de masses d'imatges, MALDI, plantes.

3. INTRODUCTION

During many years scientists, have been trying to understand the gene expression or undergoing protein analysis about the living organisms. However, they were ignoring an important question: changes in the metabolome are the ultimate answer of an organism to alterations, diseases or environmental influences [1]. Imagine a situation in which in a known pathway there is a metabolite that is not synthetized, but it should. At this point, the question is: What is wrong inside the pathway? There are many possible answers, nonetheless the important thing is that the problem has come to light thanks to the lack of this metabolite. From now on, scientists may resort to other sciences to solve this problematic. From these thought, the field of metabolomics rapidly emerged. Metabolomics combines strategies to identify and quantify metabolites which can be defined as small molecules that are chemically transformed during metabolism, so they provide a functional reading of cellular state [1].

Nowadays, a range of analytical technologies such as liquid chromatography (LC), gas chromatography (GC), matrix assisted laser desorption ionization (MALDI) coupled to a mass spectrometry (MS) and nuclear magnetic resonance (NMR) are employed to determine and quantify as many metabolites as possible, either identified or unknown in different organisms, tissues or fluids [2].

3.1. METABOLOMICS

The first approach to metabolomics traces back all the way in the ancient China when traditional Chinese doctors started using ants in order to evaluate the urine of patients to determine if it contained high glucose to detect diabetes.

Many years later, in the seventeenth century, Santorio Sanctorious published the first work (called “insensible perspiration”) in obtaining physical data and providing quantitative basis of pathology based upon precise studies and instrumentation.

Finally, in the twentieth century and with the advancements in technology the separation of metabolites to study each individually was possible enabling metabolomics. Nevertheless, it was not until the year 1998 that this term came to be used [3,4].

Currently, more than 240.000 metabolites are known including the most common biological molecules: sugars, lipids, amino-acids and nucleic-acids [3].

3.1.1. Lipidomics

The aim of metabolomics is to determine as many metabolites as possible. Due to the large diversity of metabolites that differ in structure and properties it results hard to classify all of them. So, it is habitual to simply organize them in hydrophobic metabolites referred to lipids and in hydrophilic metabolites for the rest. This fact added to the significant biological implication of this group of molecules made possible the emergence of a new independent field denominated as lipidomics [5].

There is no widely accepted definition of lipid. General text books usually describe lipids as a group of natural compounds which have in common a ready solubility in organic solvents such as alcohol or chloroform due to the fact that they are formed by hydrophobic long carbon chains [6].

They are found in all leaving species and play essential roles in cellular function including self-assembly of phospholipids to form the membrane bilayer or storing energy.

It exists a largely classification of lipids depending on their function and structure.

3.1.1.1. Fatty acids

Fatty acids are composed by a long aliphatic chain and a carboxylic acid group. They can be classified according to the presence of double bounds. Those which present that characteristic are known as unsaturated and the other saturated.

They have important functions such as building blocks of phospholipids and glycerophospholipids, targeting molecules attached to proteins, fuel molecules being stored as triacylglycerides and messenger molecules (products of fatty acids function as hormones and intracellular messengers) [7].

3.1.1.2. Sphingolipids

Sphingolipids comprise a range of lipids in which fatty acids are linked by amide bonds to a long chain (sphingosine) as shown in Figure 1.

They are mainly located in the plasma membrane of mammalian cells where they have structural function. They also act as adhesion sites for proteins and their metabolites have important roles in signal transduction [8].

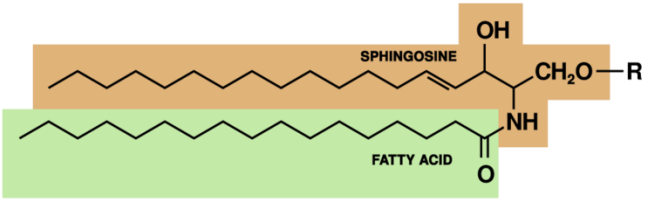

Figure 1. Sphingolipid general structure.
(Extracted from biochempages, 14/5/17)

3.1.1.3. Glycerophospholipids

This group constitutes the major class of lipids present in all cells. They are significant components of cellular membranes and are typically asymmetrically distributed across the membrane bilayer. Glycerophospholipids also act as an emulsifying agent to promote dispersal of one substance into another [9].

The general structure is shown below (Figure 2). These are structures consisting of a molecule of glycerol to which are attached two fatty acids (R1 and R2), a phosphate and usually one another small molecule (Z). Regarding to that Z group, glycerophospholipids can be classified in phosphatidylcholines, phosphatidylinisitols, phosphatidylserines, phosphatidylglycerols and phosphatidyletanolamines among others.

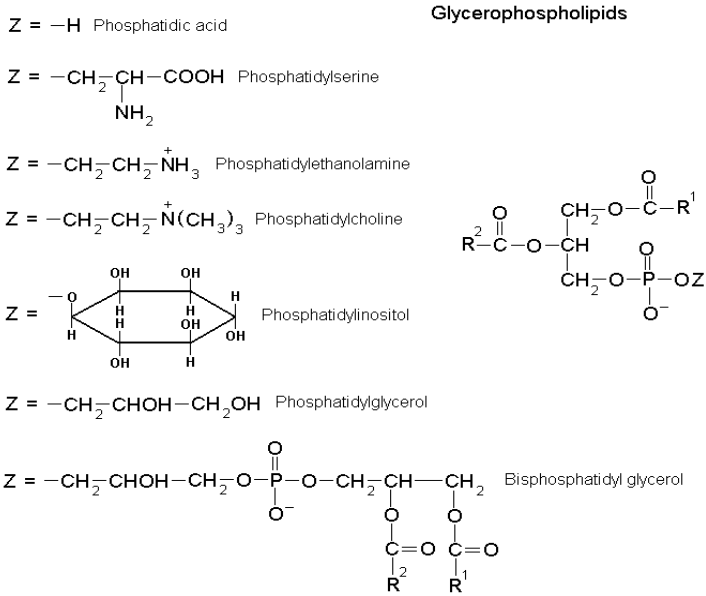

Figure 2. Glycerophospholipid general structure and examples. (Extracted from Wikipedia, 23/5/17)

3.1.1.4. Glycerolipids

Glycerolipids are composed of mono-, di- or tri-substituted glycerols. The most known function is energy storage, related to triacylglicerol, but they can also serve as signal transducers. They can also include the presence of one or more sugar residues such as in the case of galactolipids (Figure 3), a case of glycerolipids only present in plants and cyanobacteria. These includes monogalactodiacylglycerols (MGDG), digalactosyldiacylglycerols (DGDG), sulfoquinovosyldiacylglycerols (SQDG) and they are essential for the photosynthetic process.

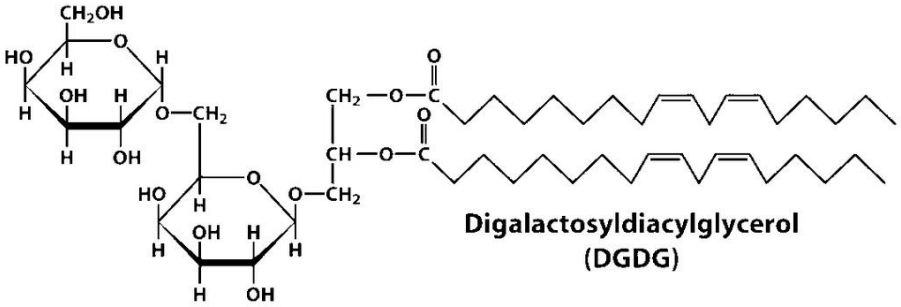

Figure 3. DGDG an example of glycerolipid.

3.1.1.5. Steroids

Steroids are organic compounds with a fused ring structure. All of them have four linked carbon rings and many of them have a short tail. They have two principal functions: some of them are important components of the cell-membranes and others are signaling molecules [10].

Some examples are cholesterol (Figure 4) or testosterone.

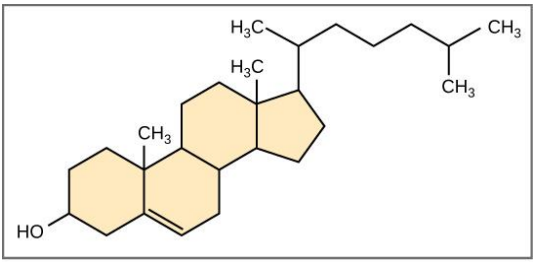

Figure 4. Cholesterol: the most common steroid. (Extracted from boundless, 14/5/17)

3.2. METABOLOMIC CHARACTERIZATION

Some difficulties are presented when the metabolome is the object of the analysis owing to the large number of metabolites presents in the organism. For these reason, two possible strategies of identification and quantification have been developed.

On the one hand, the targeted strategy is a quantitative analysis of specific and characterized metabolites in a sample. The main drawback is that other potentially interesting chemicals presents in the sample are disregarded and will not be analyzed. On the other hand, the non-targeted method considers all the full scan data obtained through different analysis techniques in order to detect both known and unknown chemicals. However, the data analysis tends to be more complex.

A large variety of analytical techniques are employed to analyze the metabolites. Some of them are GC-MS, LC-MS, MALDI-MS or NMR. This work is based in the use of MALDI-MS technique.

3.2.1. Mass spectrometry (MS)

Mass spectrometry is an extensively used analytical technique that provides molecular and atomic masses of analytes with high accuracy in a single measurement.

The most important component is the mass spectrometer which consists in three parts. The ion source where analytes are desorbed and ionized, the analyzer where they are separated according to mass charge ratios (m/z) and the detector in which the separated ions are identified and quantified by measuring the abundance of the ionized molecules or fragments. Finally, the results are displayed on a chart. Usually the highest value m/z peak is referred to as the molecular ion peak [11].

3.2.2. MS/MS

MS/MS is a technique used to break down selected ions that are characteristic of a given analyte mixture (precursors) into fragments. Once the sample is ionized to generate a mixture of ions and any of interesting m/z peak is seen, this can be fragmented to generate a product of ions for detection.

It uses two mass spectrometers in tandem and between them there is a collision gas cell. Precursor ions selected by MS collide with a high pressure gas in the cell and undergo fragmentation [12,13].

The resulting spectrum consists only of product ions from the selected precursor.

A MS/MS workflow scheme is shown in Figure 5.

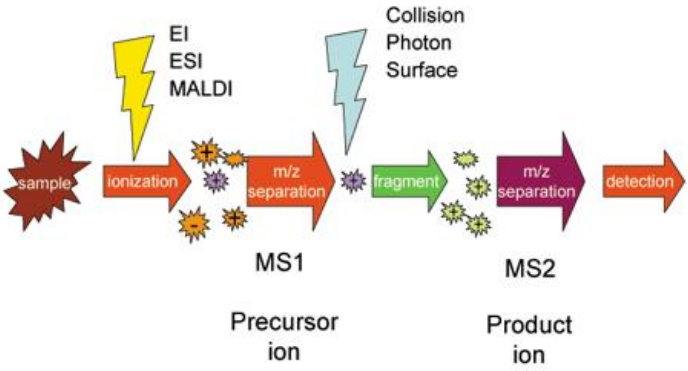

Figure 5. Mass spectrometry MS/MS workflow. (Extracted from nationalmaglab, 11/5/17)

3.2.3. Mass Spectrometry Imaging (MSI)

MSI is a label-free technique used in mass spectrometry to visualize the spatial distribution of a large variety of analytes in tissue sample surfaces. This information improves the understanding of the metabolism and the biochemical function of specific tissues.

Tissue sample area can be sectioned in small regions. Every region is denominated as “pixel”. For every pixel, the instrument collects a spectrum, then one spectrum for each pixel in the sample is recorded. The instrument undergoes an average (median) of all of them, and a general spectrum (mean spectrum) in which the intensity is shown as a function of position with the relative intensities, is plotted typically illustrated by a color scale in a 2D heat map (Figure 6). It results useful because if a concrete peak is selected, the mass distribution and intensity of this peak of the mean spectrum within the sample surface is shown.

Most MSI are performed in a full scan mode, so an entire mass spectrum is recorded in each pixel of the image, therefore all the compounds which are ionized are detected and can be imaged simultaneously.

What differs between the different MSI techniques is the method of ion generation. Some examples are by ion bombardment as in Secondary Ion Mass Spectrometry (SIMS) or by laser illumination as in Laser Desorption Ionization (LDI/MALDI).

The image resolution indicates the quality of it. It is measured with pixels per inch. To more pixels, more resolution and therefore better image quality. The problem in attempting MALDI imaging at higher resolution is the fact that ionization yield drops significantly with laser spot sizes smaller than 1 μm [14].

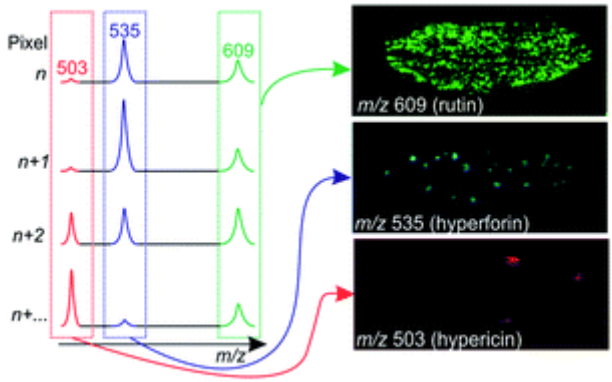

Figure 6. MSI exemple.
(Extracted from Ref. 17)

3.3. MALDI TOF

MALDI stands for Matrix-Assisted Laser Desorption Ionization and is a versatile analytical technique to detect and characterize mixtures of organic molecules such as polymers, proteins or lipids. It is a soft ionization method that involves a laser striking of a small organic molecule called matrix to form gaseous ions without fragmentation or decomposition. Matrices have in common a conjugated pi system that is able to absorb energy in the form of UV light and blast the analyte molecules into gas phase. During this process, the analyte molecules are ionized usually by proton transfer with the nearby matrix molecules. The most common ionization format is to carry a single positive or negative charge.

Once the gas-phase analyte ions are generated, their masses can be studied by the analyzer. The majority of the commercially available MALDI instruments are based on a TOF (Time of flight) mass analyzer which enclosed the sample in a vacuum chamber during the analysis and accelerates the ions in a high-voltage electric field which imparts a constant amount of kinetic energy on the ions. According to the expression $KE = 1/2mv^2$, the smallest of the ion travels the fastest [15,16].

TOF separates ions by their mass to charge ratio and determinates this parameter by the time it takes for the ions to reach the detector. Finally, a mass spectrum is recorded.

How MALDI-TOF technology works is summarized in Figure 7.

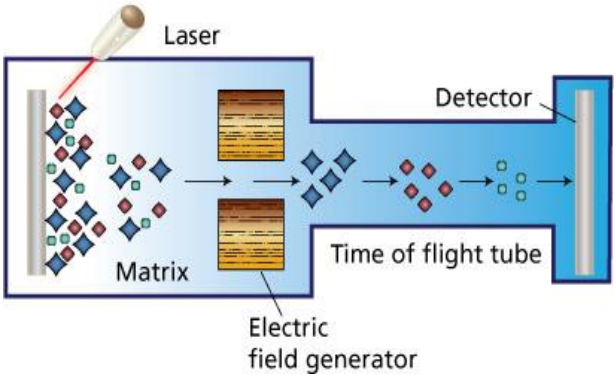

Figure 7. MALDI-TOF Technology.
(Extracted from dna-barcoding blogspot, 11/5/17)

3.3.1. MALDI Matrix

The correct choice and application of the matrix is a crucial step because it has direct consequences for the spatial resolution and the ionization efficiency of metabolites.

One defining characteristic of MALDI-TOF is the use of large nonvolatile organic molecules as matrix. There are many substances that are commonly used as a matrix. They tend to be small organic molecules with a conjugated pi system that absorbs UV light. This allows the energetically excited matrix to physically ablate the sample, carrying the analyte molecules into the gas phase along with them. They are usually acidic because this allows the analyte to become ionized by a proton transfer from the excited matrix molecule [17].

Both matrix and analyte need to be fully soluble in the matrix solvent.

Some of the most common matrices are 2,5-Dihydroxydbenzoic acid (DHB), 1,5-Diaminonaphtalene (DAN), sinapinic acid (SA) and α-cyano-4-hydroxycinnamic acid (CHCA) [17].

3.3.2. MALDI MSI workflow

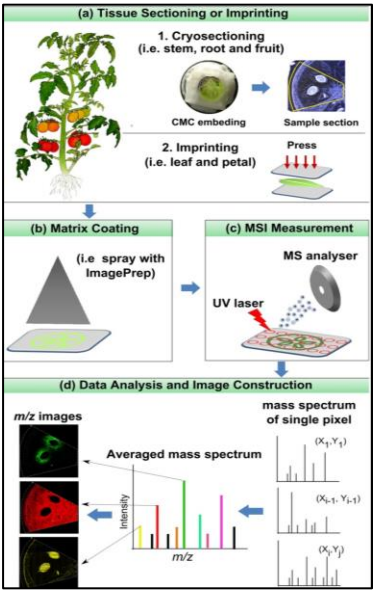

Figure 8. MALDI MSI process. (Extracted from Ref.18)

Before the MALDI analysis, it is necessary to follow an accurate process in order to prepare the sample for being studied.

As it is seen in Figure 8, the most important steps during the MSI process are the tissue preparation, the matrix application, measurement and data analysis. All of them will be explained in detail in the experimental section.

3.4. ABOUT THE STUDY

MSI is a relatively new innovative technique; consequently its application is still being studied. It is also need to say that the majority of the studies that have been done involve to mammalian tissues leaving behind the plant sciences. Nevertheless, plants undergo interesting biosynthetic processes and metabolic networks that could be used to improve many fields such as pharmaceutical, general medicine, biochemistry, etc. For these reasons, MSI has started gaining popularity in plants few years ago.

This work is focused in the study of MSI of lipids presents in plants, more precisely in green bean and rice plants. An important blind alley in non-targeted lipidomics is the identification of lipids from the m/z values obtained experimentally because the mass analyzer does not have the enough resolution, then the identification is complex. To overcome this issue, in the present work the fragmentation of some of these common lipids was carried out in order to understand the fragmentation patterns in MALDI and to elaborate a fragment database of lipids for further

identification in plant tissues. Besides, as better detection of the tissue the more signals are obtained. Hence, different strategies to improve MALDI sample preparation were developed.

4. OBJECTIVES

As it was introduced in the previous section, this work present two main objectives:

- Lipid standard fragmentation and creation of fragment databases as a tool for lipid identification using MALDI TOF/TOF instrument.
- The optimization of plant leaf samples preparation for MALDI Imaging.

5. EXPERIMENTAL SECTION

This work is divided in two differential parts according to the objectives: lipid fragmentation and optimization of sample preparation for MALDI Imaging. Although they have in common the MALDI analysis, they follow a different sample preparation process. Hence, the experimental section will be split in two parts.

5.1. LIPID FRAGMENTATION

5.1.1. Reagents

- Lipid standards

-Fatty acids: Palmitic acid, Arachidonic acid, Oleic acid, Stearic acid, Nervionic acid, Jasmonic acid and Myristic acid.

-Sphingolipids: 12:0 Sphingomyelin (SM), 12:0 Glucosylceramide (GluCer), 12:0 Ceramide (Cer), 17: 0 Sphinganine (Sa), Sulfatide and 18:0 D3 Gangliosides (GM1, GM2 and GM3).

-Phospholipids: 17:0 Lysophosphatidic acid (LysoPA), 17:1 Lysophosphatidylethanolamine (LysoPE), 17:0 Lysophosphatidylcholine (LysoPC), 17:1 Lysophosphatidylglycerol (LysoPG), 17:1 Lysophosphatidylserine (LysoPS), 16:0 D31-18:1 Phosphatidic acid (PA), 16:0 D31-18:1 Phosphatidylethanolamine (PE), 16:0 D31-18:1. Phosphatidylcholine (PC), 16:0 D31-18:1 Phosphatidylglycerol (PG), 16:0 D31-18:1 Phosphatidylserine (PS) and Cardiolipin mix (14:1(3)-15:1 CA 15:0(3)-16:1 CA 22:1(3)-14:1 CA 24:1(3)-14:1 CA).

-Glycerolipids: 17:0 Monoacylglycerol (MAG), 1,3-17:0 D5 Diacylglycerol (DAG) and 1,2,3-17:0 Triacylglycerol (TAG).

-Galactolipids: Monogalactosyldiacylglycerol (MGDG), digalactosyldiacylglycerol (DGDG) and sulfoquinovosyl diacylglycerol (SQDG).

-Steroids: 17:0 Cholesteryl ester (CE) and Hydroxycholesterol (HC).

-Prostaglandins: prostaglandin E2 (PGE2).

- Other standards:

- L-acetylcarnitine
- Chlorophyll a

- Chlorpyrifos

- Matrices:

- 2,5-Dihydroxydbenzoic acid (DHB)
- 1,5-Diaminonaphtalene (DAN)

- Solvents:

- Methanol
- Acetonitrile (ACN) and trifluoracetic acid (TFA 0,1%).

Lipid standards were provided by Avanti Polar Lipids except fatty acids which were provided by Sigma Aldrich. The other reagents, matrices and solvents were provided by Sigma Aldrich.

5.1.2. Solutions preparation

- Lipid standards preparation

The individual stock standard solutions were prepared in methanol at a concentration of 200 μM in an Eppendorf tube for each standard. All standard solutions were stored at -18ºC until use.

- Calibration mixture preparation

A solution known as peptide calibration standard mixture (Bruker) was used. It allows calibrations and testing of MALDI-TOF mass spectrometers in a mass range between 600 and 3500 KDa. The mixture, which contains seven peptide standards, was dissolved in 125 μl of TFA 0.1%/ACN 2:1. Then, it was stored in aliquots of 5 μl at -18ºC.

- Matrix preparation

To prepare the matrix for the dried droplet method, a saturated solution was prepared in an Eppendorf tube at room temperature and it was vortexed to ensure that was mixed. The components mixed were 10 mg of DHB dissolved in TA30. TA30 was prepared with acetonitrile and TFA 0.1% 70:30 [v/v]. In the case of DAN TA50 which differs with TA30 in the volume of TFA 0,1 % added (50:50 [v/v]) was used.

5.1.3. Instrumentation

Simple instrumentation

The materials and small equipment used were:

- 1.5 ml Eppendorf tube
- Vortex mixer (Scientific Industries)
- Ultrasound bath (P Selecta)
- MC 7000 centrifuge (Ibx instruments)
- 1-1000 μl micropipettes

MALDI

The system employed consists in Autoflex™ series MALDI-TOF/TOF (Bruker) equipped with an improved Smartbeam™ laser technology with up to 200 Hz repetition rate. Spectra were obtained in positive reflector ion mode in the 400 to 2000 m/z range. The TOF/TOF technology (LIFT™) enables the use of various MS/MS techniques (LID or CID).

The computer software used to control and choose the parameters of the process has been FlexControl (Bruker). For statistical analysis, spectra can be analyzed with FlexAnalysis (Bruker).

5.1.4. Matrix application

Solutions of the matrix and the analyte were loaded onto a sample plate called target. The target is made of polished or ground stainless steel and has spots for several different samples. Here, the solvent is allowed to evaporate from the solution leaving behind a solid sample spot on the target that is analyzed by the MALDI-TOF spectrometer.

In this case, a method known as dried droplet was used: 1 μL each of matrix and 1 μL of a standard lipid solution were mixed in a piece of parafilm. Then, 1 μL of the mixture was drop onto a sample spot of the target with a micropipette. The same process was also done with the calibrant mixed with the matrix.

Figure 9 shows how the matrix and the sample are deposited into the target forming visible white crystals.

Two different matrices were used in this experiment: DAN and DHB. Both are valid for lipid research.

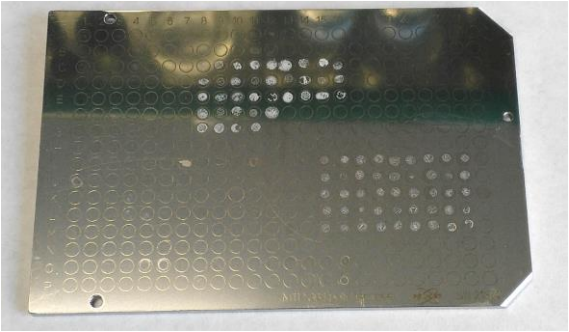

Figure 9. MALDI target dried droplet method.

5.1.5. Maldi analysis

Before the analysis, the calibration of the instrument and setting of some parameters is required. MALDI software has an automatic system of the standard mixture detection. Once the calibration was done, the sample could be analyzed. As it is a targeted analysis, there is a different known mass for each lipid standard, so the mass rank introduced will be also different but always within the characteristic lipid mass rank (200-1200 KDa). The power striking laser was established between 50-70%.

In order to carry out the MS/MS fragmentation the LIFT method was used in which it was introduced the mass parent ion that was fragmented into more m/z peaks.

5.2. OPTIMIZATION OF IMAGING SAMPLE PREPARATION

5.2.1. Materials and reagents

- Plants: green bean and rice.

In this part, the experiment was carried out with green bean and rice plants already grown for other ongoing research in the host laboratory. Briefly, green bean plants were previously treated with 0.5 mg/g soil pesticide (Chlorpyrifos) and others were grown at normal conditions (control). Both were watered and exposed to the sunlight next to a window during 60 days. The leaves used for the present study were collected and stored in a tube at -18ºC.

Regarding rice plants, they were grown in a plant chamber and watered with Cu and Cd at concentrations of 50 and 1000 ppm and stored in a tube at -80ºC to preserve them and avoid metabolism activity.

- Sample preparation materials:
    - Indium-tin oxide (ITO) glass slides.
    - Matrix: 2,5-Dihydroxydbenzoic acid (DHB) and 1,5-Diaminonaphtalene (DAN).
    - Solvents: acetone.
    - Sublimation equipment: heating plate, sand bath, thermometer, glass sublimator, vacuum pump and doubled sided tape.
    - Other: metallic block and carbon double coated conductive tape.

5.2.2. Sample preparation details

5.2.2.1. Indium-tin oxide (ITO) glass slide preparation

Indium-tin oxide (ITO) glass slides sample plates are slides coated with indium-tin oxide on one surface to provide a conductive surface and marked for MALDI Imaging.

The first step in MALDI Imaging sample preparation is placing the tissue onto the ITO. The most common method used is cryo-sectioning which consists in cutting the tissue in thin slices (10 to 20 μm) that attach themselves into the slide. Sample size and shape are factors that need to be considered and leaves are thin and fragile tissues, hence are a challenge to cut in sections. The resulting surface is not generally flat and then, the instrument has difficulties in sample detection.

The main objective was to improve and facilitate the way the sample is deposited onto the ITO slide. To achieve it two different experiments were tried: sample imprinting in which plant tissues were pressed onto the ITO slide transferring the plant metabolites at different conditions and conductive tape sample attaching. The first step of the process was common in both experiments and it was as follows: first, four cross marks were made in the respective corners of the ITO slide using Tipp-Ex. Then, the sample was placed onto the slide and its shape contoured. Afterwards, a picture was taken with a 13 Megapixel mobile camera (Huawei G7) to further co-localize image to the sample introduced in MALDI instrument. This process is called *teaching*.

Imprinting improvement

In the case of imprinting, first of all, leaves were placed in filter paper. After, the ITO was positioned above them carefully and ensuring that the surface was flat at every moment. Then a uniform and constant pressure was needed to imprint leaf metabolites into the slide. For that task, a metallic block which has a flat surface during five minutes was utilized.

To improve the signals obtained with this method, different imprinting conditions were tested (Figure 10). Two ITO slides were employed at the same time with two control leaves on each. The situations tested are:

- ITO 1: Use of MeOH. A sheet of filter paper was impregnated with methanol and one leaf was placed above. Both were at room temperature.
- ITO 2: Use of MeOH and temperature. The application of MeOH was the same as in ITO 1. Both were at 40ºC. To achieve this temperature, the pressure upon the slide was made with a metallic block previously heated with a hot plate at this temperature.

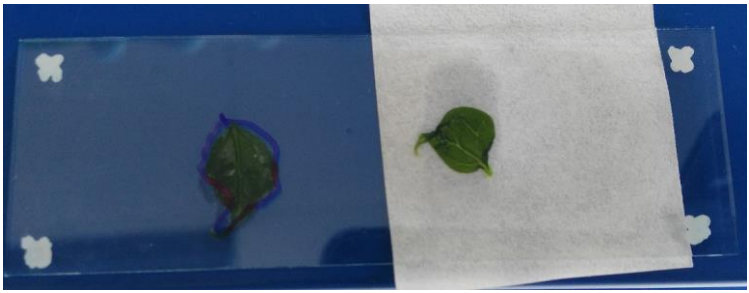

Figure 10. An example of ITO slide procedure with green bean leaves.

Use of conductive tape

The second experiment was carried out with carbon double coated conductive tape (TED PELLA, INC.). It was directly sticked into the ITO slide. Thus, tissue sample was placed onto the tape (Figure 11 and 12) and it was not required to exert any force due to the fact that there was no need of tissue impregnation. In this case, contaminated and control sample are both tested.

Figure 11. Rice plants tape doable coated tape experiment.

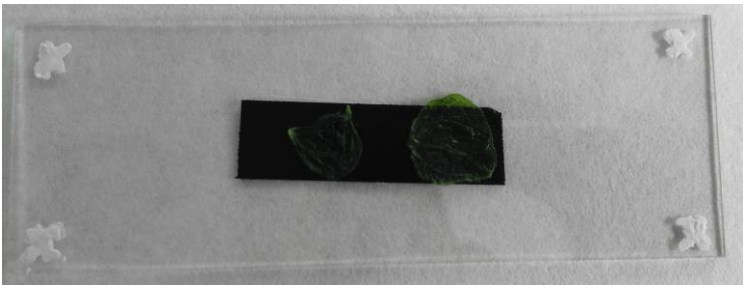

Figure 12.Green bean leaves tape experiment.

5.2.2.2. Sublimation

MALDI matrix can be deposited on tissue in several ways. Sublimation was the method chosen for this work. It allows fast and uniform matrix deposition without decomposition under conditions of reduced pressure and elevated temperature.

The sublimation device is composed by two principal parts: the condenser and a flask with flat bottom. These two, are assembled with an O-ring seal and connected to a direct drive vacuum pump.

First of all, 10 mg of the matrix were dispersed homogenously in a Petri dish with acetone. The solvent was evaporated during 15 minutes in a fume hood and put into the flat bottom flask. In the inner-bottom part of the condenser, the ITO slide was fixed using double sided tape (Figure 13). The system was closed using the O-ring joining the two parts of the sublimator device which was placed in a sand bath necessary for the homogeneous heat distribution. Then, the vacuum pump was connected and finally, water was poured into the condenser as cooling substance. The entire assembly can be seen in Figure 14.

The temperature was set at 145ºC; however, sublimation begins a few degrees below (between 140-143ºC). This process lasts about 10-15 minutes and it is stopped when the ITO slide turns white due to the matrix condensation.

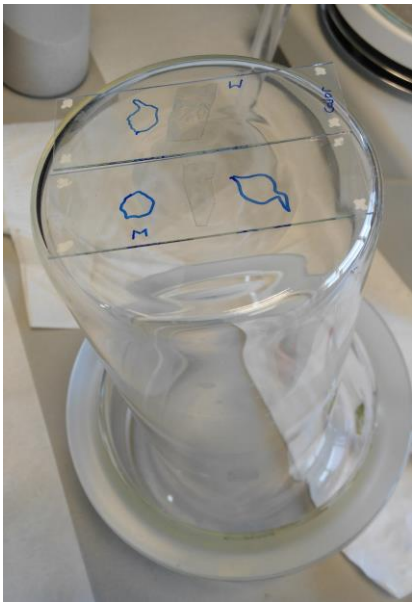

Figure 13. ITO slide attaching.

Figure 14. Sublimation assembly.

.

5.2.3. MALDI analysis

MALDI System employed was the same as in experimental part 1. Laser raster was set to 150 μm along both x-axis and y-axis. Regarding to the software, in this part there is included another one: FlexImaging (Bruker) used for imaging data acquisition analysis. Thanks to the four cross marks in the ITO slide and the teaching process to delimitate the work area, MALDI is able to co-localize the image seen in the screen to the sample introduced in the instrument.

5.3. DATA ANALYSIS

When the objects of the study are the standard lipids a targeted analysis was carried out due to the fact that the searched mass was previously known. Then, when the sample was analyzed

a mass spectrum which represents the intensity of each m/z plot was obtained. Hence, the distribution of ions by mass was obtained. In this case, the peak with major intensity always corresponds to the standard lipid mass.

The following step consists in the fragmentation of these standards which provide another mass spectrum containing the mass fragments.

In order to relate every peak in the second mass spectrum with the correspondent ion structure the software ChemDraw was used. This allows drawing the molecule and with the tool "fragmentation", obtaining the mass of every possible fragment.

Normally, fragments are not identified as themselves owing to the fact that they form adducts with other ions on the medium. So, the mass detected is not the same. The most common adducts are with H^+, H^-, Na^+ or H_2O.

With all the information extracted, tables with characteristic peak fragmentations of every standard lipid were elaborated.

When the experiment is done with green bean or rice plant tissue the analysis is untargeted. Then, the analysis process was the same as before, but with the difference that in the spectra there were more molecules aside of lipids and all of them were unknown. Then, the peaks of the tissue were fragmented in order to obtain a fragment spectrum of each one for its further identification.

In order to ease the peak identification there are metabolomic data bases such as METLIN, HMDB or LIPID MAPS which have registered a huge amount of metabolites. Thus, mass peaks are introduced and they give a list with all the possible metabolites. This, together with the use of the fragment tables, enabled the identification of lipids in the sample.

Regarding the image distribution of the metabolites within the tissue, SCILS (Bruker) software allows seeing the mass distribution in the image of a chosen m/z in a mean spectrum. In order to simplify the results and to recognize which are the most important distributions and weights that represent the tissue, a multivariate data analysis is required. Principal component analysis (PCA) is a multivariate data analysis that extracts the most important information from the data. It enables to represent a data in a reduced dimension plane dropping the number of variables. This representation is done by deconstructing the initial variables into new ones called principal components (PC). They are the underlying structure in the data, where it is more spread out. The

first PC describes the greatest source of variability. Another application of PCA is to identify patterns in data and expressing the data in such a way as to highlight their similarities and differences among samples. The main goal is to describe as much of the information in the system as possible in the fewest number of PCs. This information is graphically visualized in scores plot which provides a map of the samples and loadings plot with variables.

6. LIPID FRAGMENTATION: RESULTS AND DISCUSSION

All the standard lipid solutions were deposited onto the target and analyzed in MALDI-TOF/TOF with the two different matrices (DHB and DAN). Some of them were seen in just one type of matrix, one ionization mode or even could not be detected. This information has been compiled in table 1. Those lipids which were not detected had not been included in the table.

Common name	Precursor ion (m/z)	Ionization mode		Adduct	Matrix	
		Positive	Negative		DHB	DAN
MAG	367	✓	×	$[M+Na]^+$	✓	✓
Lyso PA	423	×	✓	[M+Na-H]	✓	✓
Lyso PE	464	×	✓	$[M-H]^-$	✓	✓
Lyso PC	510	✓	×	$[M+H]^+$	✓	✓
Lyso PG	495	×	✓	$[M-H]^-$	✓	✓
Lyso PS	508	×	✓	$[M-H]^-$	✓	✓
PA	728*/704	✓	✓	$[M+Na]^+/[M-H]^-$	✓	✓
PE	747	×	✓	$[M-H]^-$	×	✓
PC	791	✓	×	$[M+H]^+$	✓	✓
PG	802*/778	✓	✓	$[M+Na]^+/[M-H]^-$	✓	✓
PS	815*/791	✓	✓	$[M+Na]^+/[M-H]^-$	✓	✓
CE	645	×	✓	$[M-H]^-$	×	✓
SM	648	✓	×	$[M+H]^+$	✓	✓
GluCer	642	×	✓	$[M-H]^-$	×	✓

Cer	504/480**	✓	✓	$[M+Na]^+/[M-H]^-$	✓	✓
Arachidonic	302	×	✓	$[M-H]^-$	×	✓
Oleic	280	×	✓	$[M-H]^-$	×	✓
Stearic	282	×	✓	$[M-H]^-$	×	✓
Nervionic	365	×	✓	$[M-H]^-$	×	✓
HC	409	×	✓	$[M-H]^-$	✓	×
L-carnitine	344	✓	×	$[M+H]^+$	✓	✓
CPF	348	×	✓	$[M-H]^-$	✓	×
Chlorophyll	872/871	✓	✓	$[M-Mg+H]^+$	✓	✓
Sa	368	✓	×	$[M+H]^+$	✓	×
Sulfatide	792	×	✓	$[M-H]^-$	-	✓
MGDG	769	✓	×	$[M+Na]^+$	✓	-
DGDG	932	✓	×	$[M+Na]^+$	✓	-
SQDG	862	✓	×	$[M+2Na]^+$	✓	-

Table 1. MALDI lipid detection.
*(a) *Only DHB*
*(b) **Only DAN*

From table 1 were deduced which are the best conditions to undergo the experiment and how the ions are detected (type of adduct). As it can be seen in table 1, some lipids are only visible in one ionization mode. Then, both modes are employed in each experiment. In terms of the matrix, DAN achieves better results than DHB.

At the same time, detected standards were straight submitted to MS/MS fragmentation in both matrices. M/z peaks detected and assigned to their fragment mass are shown in tables below:

Lipids not detected: GM1, GM2, GM3 DAG, TAG and PGE2.

Fatty acids: any characteristic peaks were seen.

Sphingolipids (table 2):

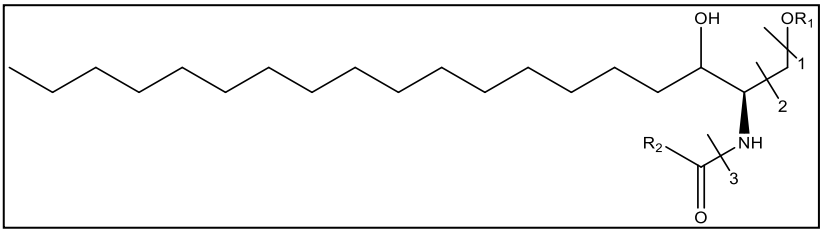

Fragment	Sphingomyelin	Glucosylceramide	Ceramide
1	182	179	-
2	-	-	31
3	*	*	*

Table 2. m/z values of sphingolipids fragments.
(a) Fragmentation depends on R2 carbon chain*
(b) R1:
-Sphingomyelin: phosphocholine
-Glucosylceramide: glucose
-Ceramide: hidrogen

Apart from the peaks from fragments 1, 2 and 3 other lipid mass peaks were also shown in the correspondent lipid spectra.

- Sphingomyelin:

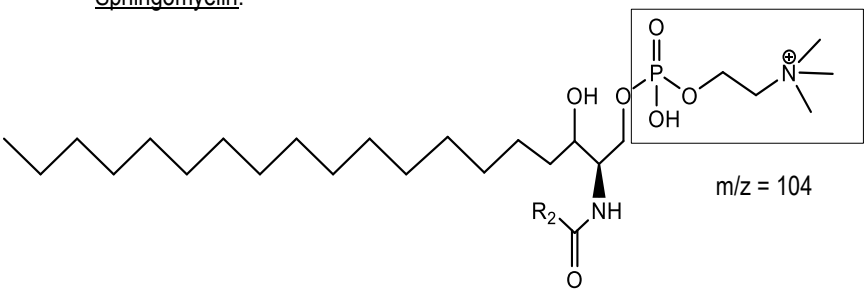

Figure 15. Sphingomyelin general structure.

- Sulfatide

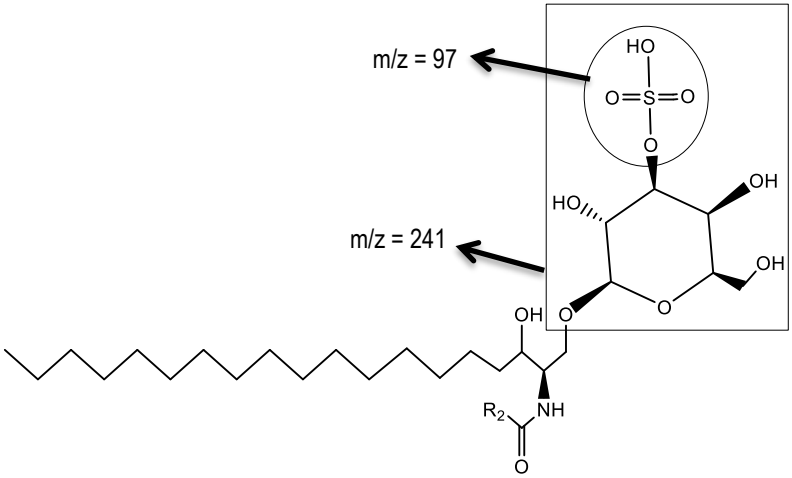

Figure 16. Sulfatide general structure.

Phospholipids

- Lysoglycerophospholipids (table 3):

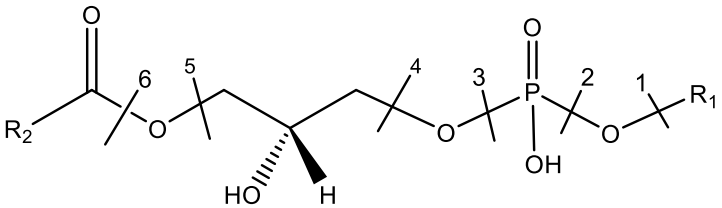

R1	H	$(CH2)_2NH_2$	$(CH2)_2N(CH3)_3$	$(CH2)_3(OH)_2$	$CH_2CHNH_3COO^-$
Fragment	LysoPA	LysoPE	LysoPC	LysoPG	LysoPS
1	-	-	-	75	89
2	-	66	104	-	-
3	81	-	-	154	-
4	98	141	182	-	-
5	154	197	-	228	-
6	171	215	-	246	-

Table 3. m/z values of lysoglycerophospholipids fragments.

Fragments $N(CH_3)_3$ and $(CH_2)N(CH_3)_3$ corresponding to LysoPC were also seen in spectra at m/z = 59 and m/z = 73, respectively. It was also observed the $[C_2H_3O_2]^{2-}$ fragment from LysoPG at m/z = 59.

R2 is referred to the long carbon chain.

- Glycerophospholipids (table 4):

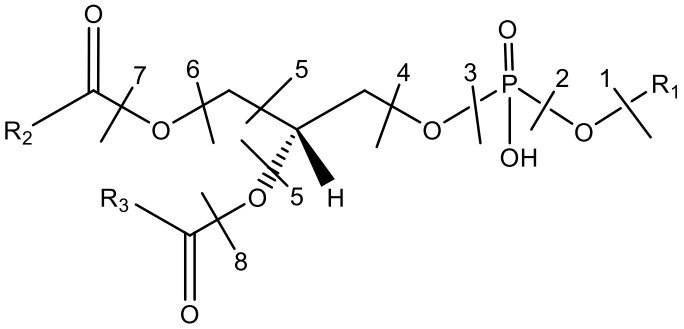

R1	H	$(CH2)_2NH_2$	$(CH2)_2N(CH3)_3$	$(CH2)_3(OH)_2$	$CH_2CHNH_3COO^-$
Fragment	PA	PE	PC	PG	PS
1	-	-	87	75	-
2	-	-	103	-	-
3	81	124	-	154	-
4	96	140	182	170	-
5+7	153	198	-	227	-
5+5	123	-	-	-	-

Table 4. m/z values of glycerophospholipids fragments.

Fragments $N(CH_3)_3$ and $(CH_2)N(CH_3)_3$ corresponding to PC were also seen in spectrums at m/z = 59 and m/z = 73, respectively. It was also observed the $[C_2H_3O_2]^{2-}$ fragment from PG at m/z = 59.

R2 and R3 are referred to the long carbon chain.

Glycerolipids

- MAG: any characteristic fragment was seen.
- DAG: any characteristic fragment was seen.
- TAG: any characteristic fragment was seen.
- Galactolipids:
    - Sulfoquinovosyl diacylglycerol (table 5):

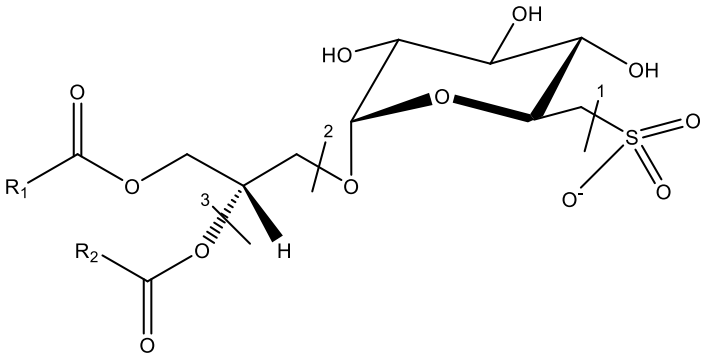

Fragment	SQDG
1	126 ($2Na^+$)
1+2	184 (Na^+)
3	*

Table 2. m/z values of SQDG fragments.
*(a) *It depends on R2*

Fragments were seen forming adducts with Na^+, except in the case of fragmentation 1 that formed adduct with $2Na^+$.

- Digalactosyldiacylglycerol (table 6):

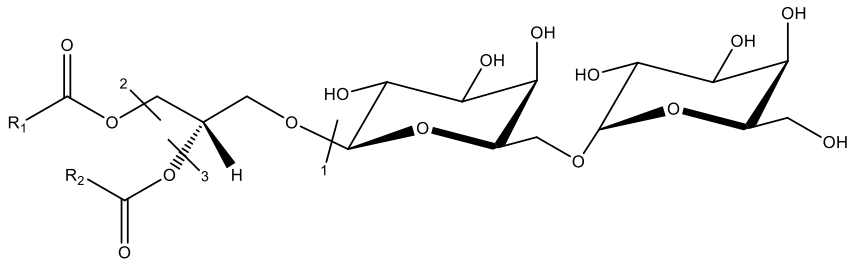

m/z	DGDG
1	347 (Na^+)
2+3	405 (Na^+)
3	*

Table 3. m/z values of DGDG fragments.
*(a) *It depends on R2*

Fragments were seen forming adducts with Na^+.

- Monogalactosyldiacylglycerol: any characteristic fragment was seen.

Stereoids:

- Hydroxycholesterol:

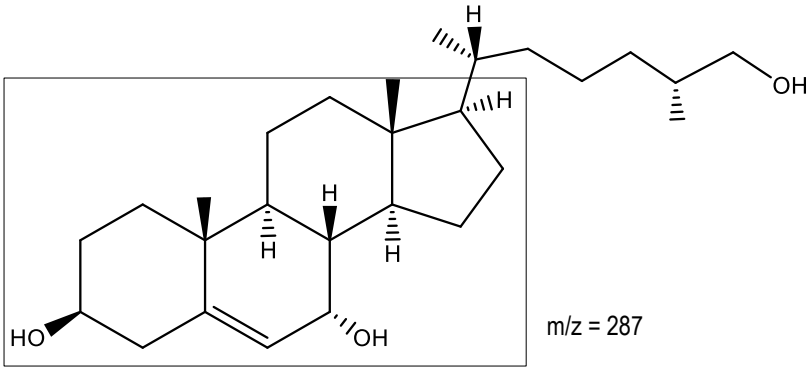

Figure 18. Dihidroxycholesterol general structure.

- Cholesteryl ester: any characteristic fragment was seen.

Other reagents:

- L-Acetylcarnitine (table 7):

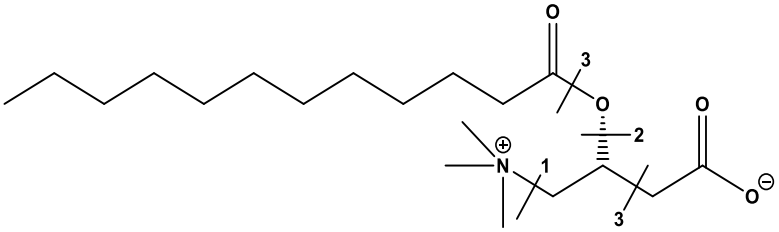

Fragment	L-acetylcarnitine
1	61
2	144
3	105
1+2	86

Table 4. m/z values of L-acetylcarnitine fragments.

- CPF: any characteristic fragment was seen.
- Chlorophyll a: any characteristic fragment was identified but it is possible to distinguish chlorophyll a from other metabolites due to its characteristically mass m/z = 871 that results from the loss of Mg^{2+} and peaks m/z = 533 and m/z = 593 which are coincident in all chlorophyll a fragmentation spectra undergone.

Furthermore, in order to identify lipids from peaks obtained through MALDI in new sample, tables with theoretical fragmentation considering the possible different acyl chain (R2 and R3) lengths were built (Appendix 1).

7. OPTIMIZATION OF MALDI IMAGING SAMPLE PREPARATION: RESULTS AND DISCUSSION

The MALDI parameters optimized for the detection and fragmentation of lipids in the previous section were applied in tissue sample detection. However, the results were not the expected when using DAN matrix in tissue sample, signals were not obtained, and then the optimization experiments were carried out with DHB matrix.

After trying the two possible experiments (imprinting and conductive tape) to improve MALDI-TOF sample detection, the best option was conductive tape. This was the way that more peaks were detected as it is shown below in Figure 18.

Figure 18 corresponds to control green bean leaves. Leaves with and without methanol and temperature and leaves with and without methanol at room temperature do not present peaks between 600 and 950 which is the common lipid mass rank. In addition, peaks between 250 and 450 are typically from DHB matrix. Nevertheless, in the case of the use of conductive tape, there are signals inside the lipids rank mass.

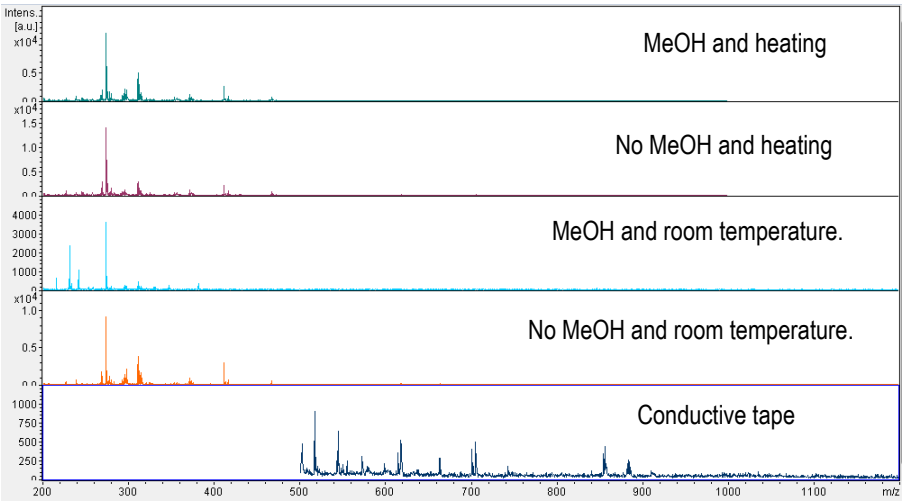

Figure 18. Comparison: spectra of Imaging and conductive tape methods.

It was also observed that with conductive tape it was needed to work in positive mode, due to negative almost did not detect peaks.

Once the best conditions were known, the lipid identification in plant tissue was carried out.

As this work is based in lipid identification, the m/z rank was bounded between 600 and 950.

Lipid image analysis of green bean leaves

The general spectrum obtained from green bean control and Chlorpyrifos leaves is shown in Figure 19. It was also observed how different mass peaks between control and CPF leaves were.

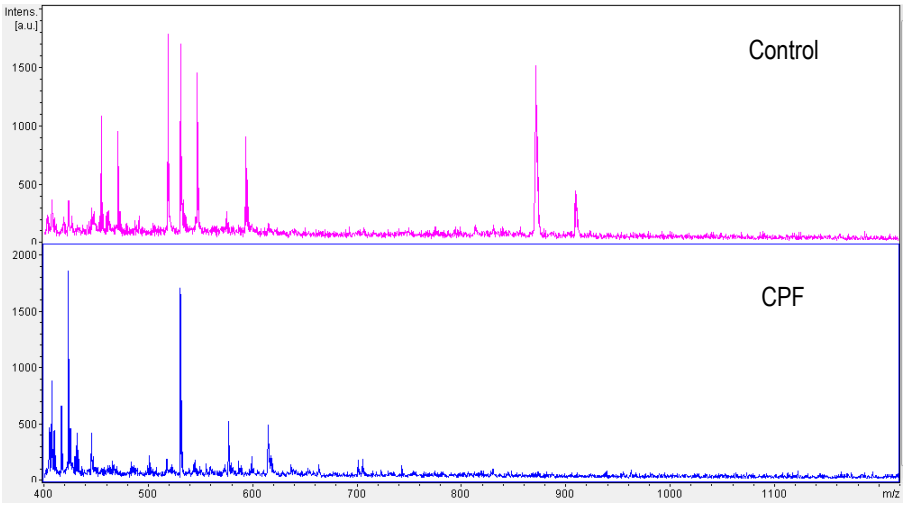

Figure 19. CPF and control green bean leaves spectra.

From these spectra, the fragmentations of the most representative peaks were done.

Afterwards, the image was carried out. In figure 20 green bean leaves are exposed as a template.

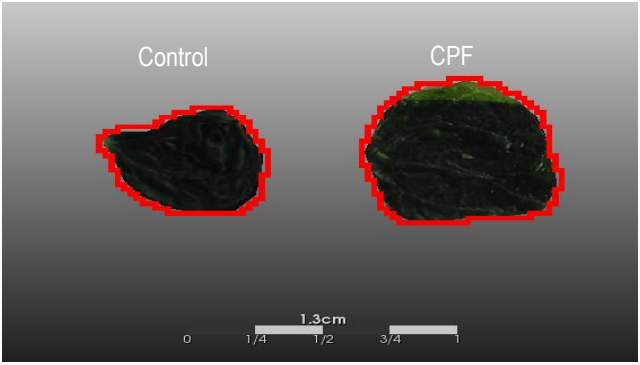

Figure 20. CPF and control green bean template.

With the information extracted from the spectra, tables and data bases the lipid identification was undergone. Some peaks were fragmented and identified:

m/z = 615 (Figure 21)

- m/z = 75

Characteristic LysoPG/PG fragment (table 3 and 4). Due to the low mass, the options decrease to LysoPG.

- m/z = 424 C24:0 (appendix 1).

The lipid proposed is **LysoPG (24:0).**

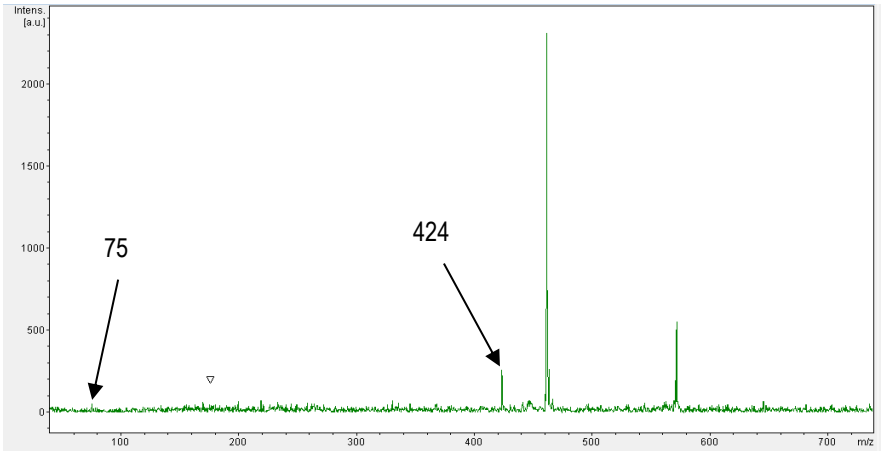

Figure 21 m/z = 615 MS/MS spectrum.

Peak mass distribution is not much relevant, but as seen in figure 22, the lipid is more present in CPF leaf and has higher intensity at the bottom of the leaf, which corresponds to the most distal part.

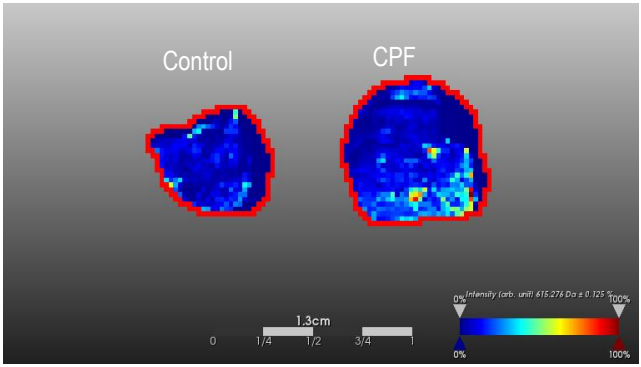

Figure 22. m/z = 615 mass distribution.

m/z = 663 (Figure 23)

- m/z = 104
- m/z = 184
- m/z = 556 C16:3 (Appendix 1)

Both fragments are common in PC and SM lipids (table 2,4). To differ between them it is applied the nitrogen rule which says that if a compound has an odd mass, it contains an even number of nitrogen atoms. However, if the mass is even, it can contain an odd number of nitrogen atoms or any. Applying this rule, the lipid must be PC.

The lipid proposed is **PC (18:3-16:3).**

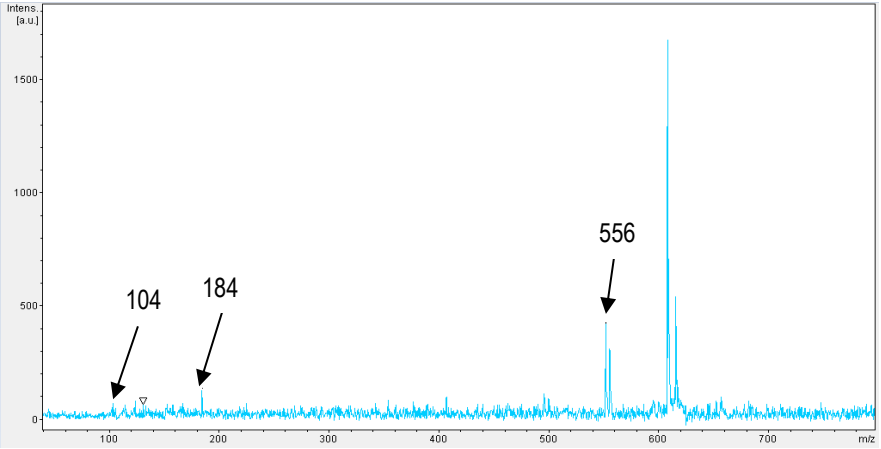

Figure 23. m/z = 663 MS/MS spectrum.

According to its image (Figure 24), the lipid is more present in CPF sample. Besides, the signal is more intense in the upper part of the leaf.

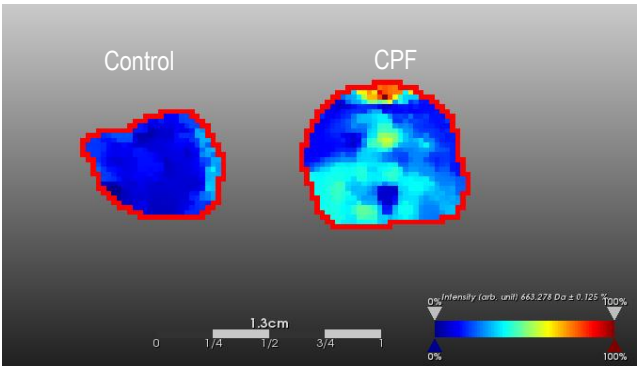

Figure 24. m/z = 663 mass distribution.

m/z = 830 (Figure 25)

- m/z = 126 (table 5)
- m/z = 184 (table 5)

These fragments are characteristics from SQDG

- m/z = 563 C16:0 (Appendix 1)

According to this information, the lipid proposed is **SQDG (16:0-18:1).**

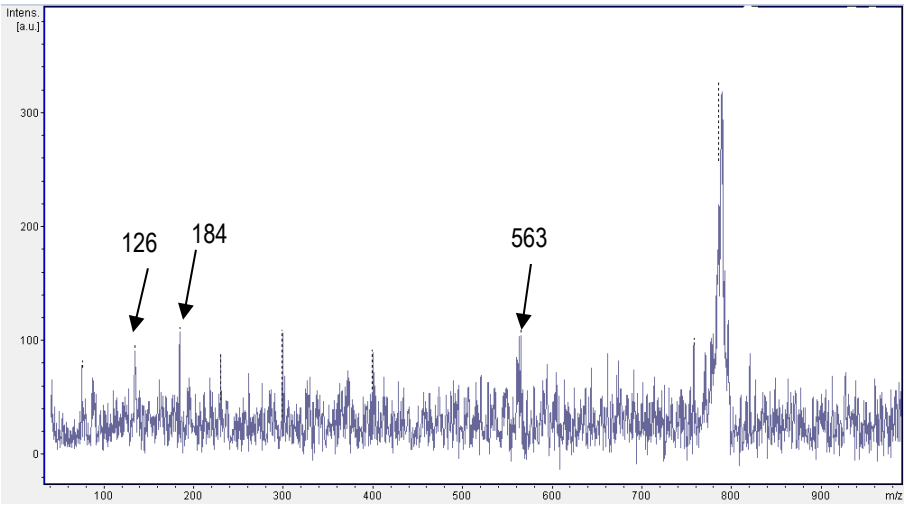

Figure 25. m/z = 830 MS/MS spectrum.

Regarding to its distribution (Figure 26), the lipid is concentrated in the middle with higher intensity in CPF.

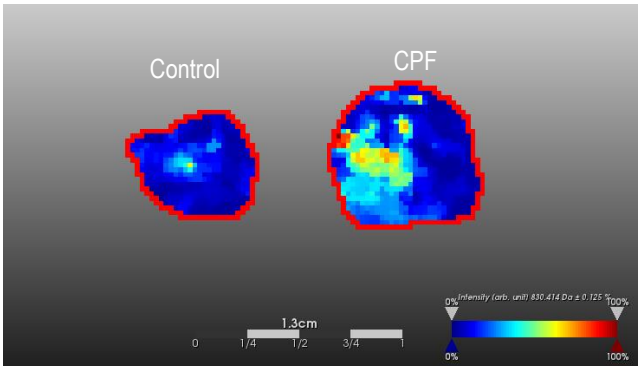

Figure 26. m/z = 830 mass Distribution.

m/z = 871 (Figure 27)

- m/z = 533
- m/z = 593

Fragments seen in Figure 27 are typically in **chlorophyll a** fragmentation. In addition, the parent mass ion coincides with its mass considering the loss of Mg^{2+} ion.

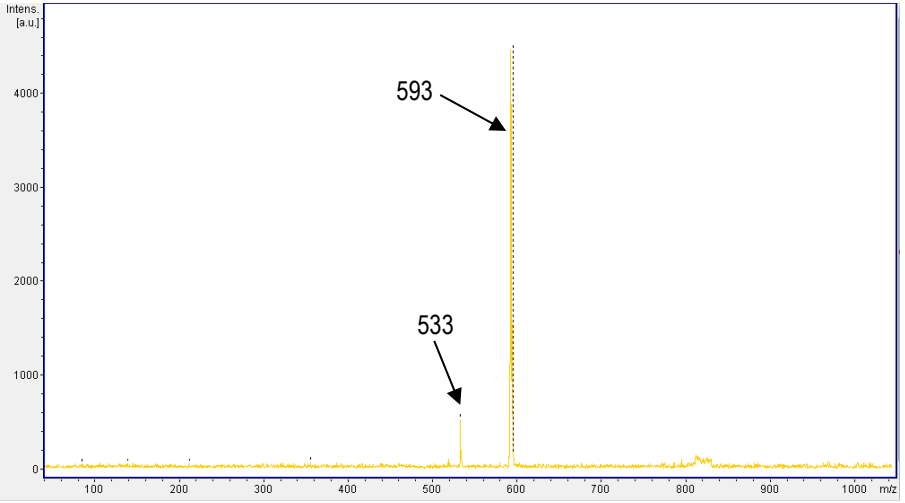

Figure 27. m/z = 871 MS/MS spectrum.

In Figure 28 it is shown how chlorophyll a is just seen in control leaf and it is distributed in whole tissue. This fact is not totally accorded with tissue due to CPF sample used was green, then this pigmentation should be contributed by chlorophyll. However, it is observed that the treatment affects the quantity of chlorophyll a in leaves.

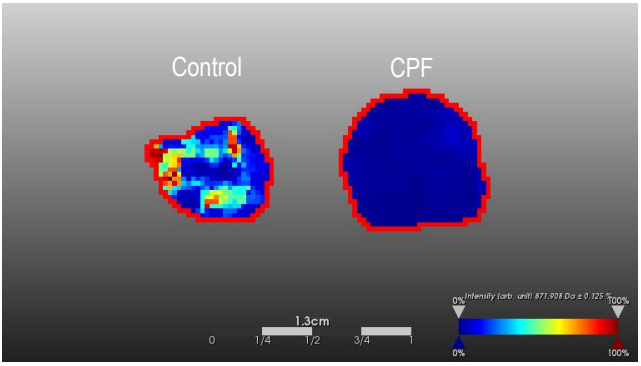

Figure 28 m/z = 871 mass distribution.

Lipid image analysis of rice leaves

The general spectrum obtained from rice leaves is shown in Figure 29. Similarities between control and treated leaves spectra are seen.

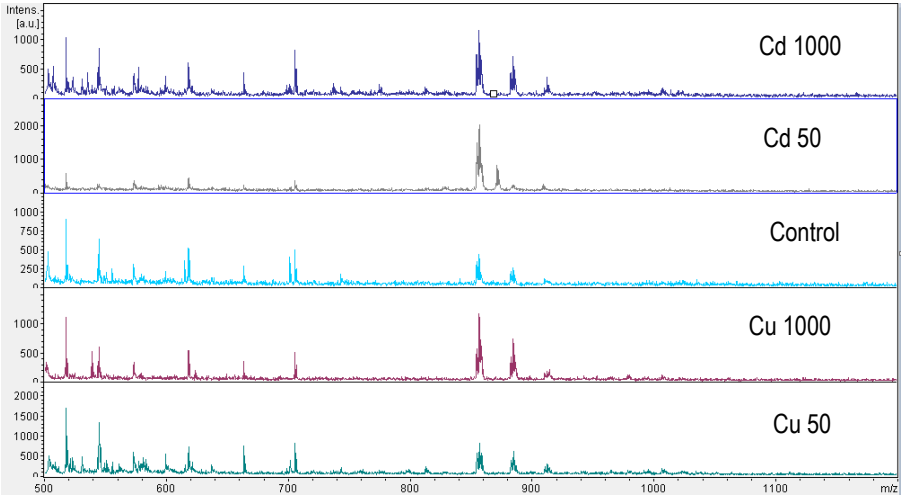

Figure 29. Rice leaves contaminated and control.

Control leaf is related to both treatments.

From these spectra, the fragmentations of the most representative peaks were done.

Afterwards, the image was carried out. In figure 30 rice leaves are exposed as a template.

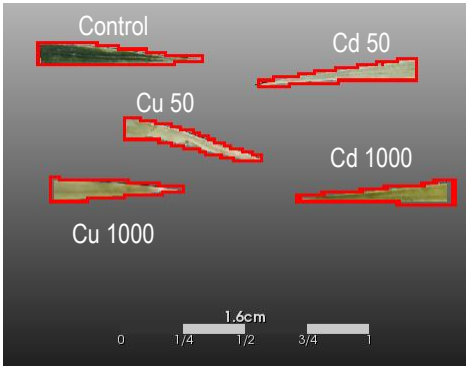

Figure 30. Rice leaves contaminated and control.

m/z = 663 (Figure 31)

This peak mass coincides with green bean. Then, the proposed lipid is the same as in the previous section: **PC (18:3-16:3).**

The mass distribution has an upward trend and the intensity increases as the concentration also does it.

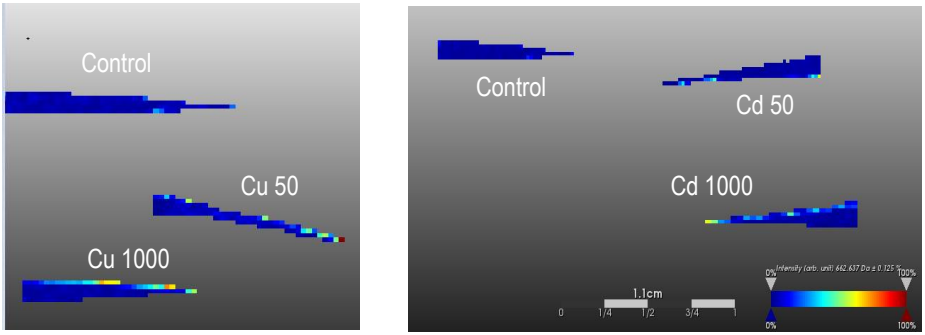

Figure 31. Distribution of m/z = 663 in rice leaves.

m/z = 857 (Figure 32)

- m/z = 59 ($[C_2H_3O_2]^{2-}$)
- m/z = 75 (table 2)

These fragments are characteristic from PG.

- m/z = 477 C16:3 (Appendix 1)
- m/z = 654 C18:1 (Appendix 1)

With this information, the proposed lipid is **PG 16:1-18:1.**

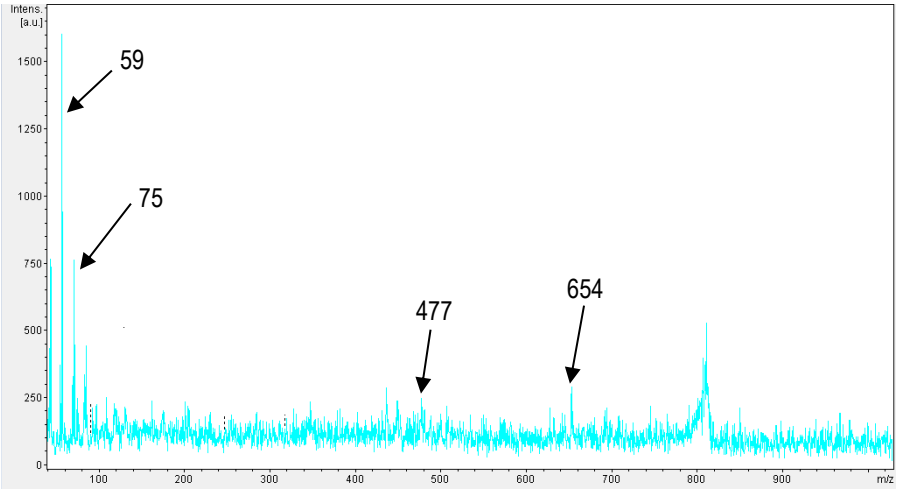

Figure 32. Rice leaves spectra at m/z = 857.

Regarding to the peak distribution it is clearly shown that PG is present in control leaf and decreases as the pollutant concentration rises. It has a constant trend.

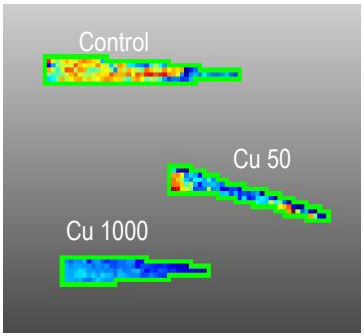

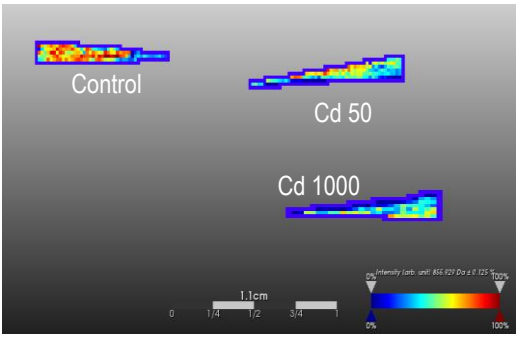

Figure 33. Distribution of m/z = 857 in rice leaves.

m/z = 883 (Figure 34)

Both spectrum and image are very similar to m/z = 857. The characteristic fragments are the same.

- m/z = 593 C24:1 (Appendix 1)

Then, the lipid proposed is **PG 24:1-20:2.**

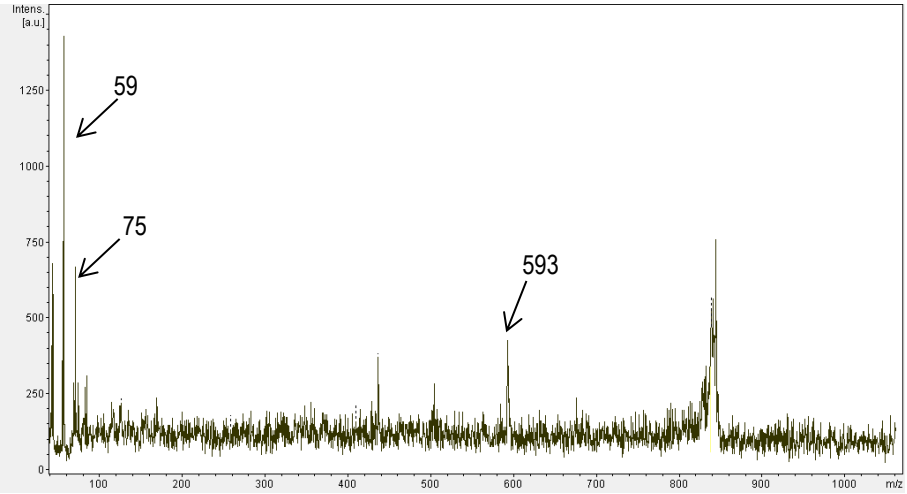

Figure 34. Rice leaves contaminated and control m/z = 883.

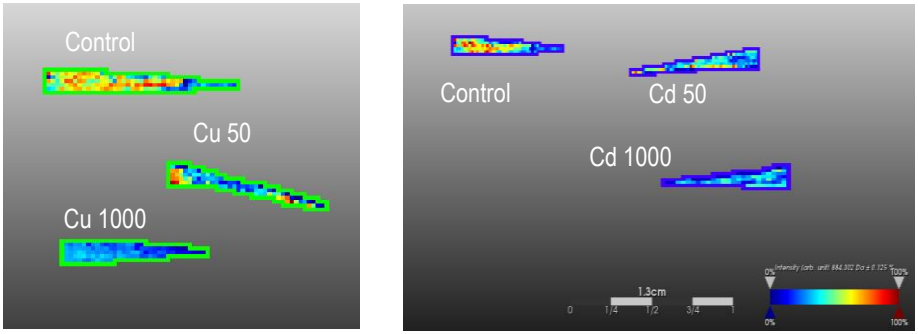

Figure 35. Distribution of m/z = 883 in rice leaves.

The metabolites identified in rice and green bean plants are mostly components implicated in photosynthesis. In addition, the distribution and intensity of these molecules vary in function of the treatment applied. In general, as the contaminant concentration rises, the abundance of metabolite decreases. Therefore, it is observed that the contaminant treatment results in an unfavorable repercussion to photosynthetic process in plants.

8. CONCLUSIONS

The main conclusions extracted from the project are the following:

- Carbon double coated conductive tape has resulted the best method for MALDI Imaging sample preparation instead of imprinting method. However, signals are just detected in positive ionization mode.
- A lipid fragmentation data base has been built. It allowed to identify lipids of leaves treated and not treated samples. Nevertheless, it is a rough job looking after m/z peaks due to the length of some tables.
- After image analysis, differences between control and treated leaves in green bean and rice plants were detected. In the case of rice plants, it has been observed that the rise of contaminant concentration affects negatively to the plant. Finally, as mostly metabolites identified are related to photosynthesis, it has been deduced that this process is affected by the contaminant treatment.

A possible investigation line to complete this work could be improving the MALDI Imaging sample preparation. It would be suggested to achieve a method which would be able to detect signals in positive and negative ionization mode at the same time.

9. REFERENCES AND NOTES

1. Dettmer, K; Hammock, B.D; Metabolomics: A new exciting Field within the "omics" Sciences. Environmental Health Perspectives. **2004,** 112(7), A 397.
2. Metz,T.O; Zhang, Q; Shen, Y; The future of chromatography-mass spectrometry in metabolic profiling and metabolomic studies for biomarker discovery. Biomark med. **2007** 1(1) 159-185.
3. Smith, Y. History of metabolomics. News Medical Life Science [Online] **2017** http://www.news-medical.net/life-sciences/History-of-Metabolomics.aspx (accessed April 13, 2017)
4. Quinlyn A.S; Dean P.J; Promislow.D.L.E. A network perspective of metabolism and aging. Integr Comp Biol **2010** 50(5) 844-854.
5. Checa,A; Bedia,C; Jaumot.J. Lipidomic data analysis: Tutorial, practical guidelines and applications. Analytica Chimica Acta. **2015**
6. Gidez, L.I. The lore of lipids. *J. Lipid Res*., **25**, 1430-1436 (1984).
7. Marshall.B. How fats work. [Online] **2000** http://science.howstuffworks.com/innovation/edible-innovations/fat.htm (accessed April 15,2017)
8. CR Gault, LM Obeid, and YA Hannun. An overview of sphingolipid metabolism: from synthesis to breakdown. Adv Exp Med Biol. **2010 6**88, 1-23.
9. Farooqui A.A; Glycerophospholipids eLS **2014**
10 K Bloch. Sterol molecule: structure, biosynthesis, and function. Elsevier **1992**
11. Glish, G.L; Vachet, R.W. The basics of mass spectrometry in the twenty-first century. Nature Reviews Drug Discovery. **2003 2** 140-150.
12. B. J. Bythell, et al, Relative stability of peptide sequence ions generated by tandem mass spectrometry. Journal of the American Society for Mass Spectrometry. **2012** 23(4) 644-654.
13. JEOL Mass Spectrometers. Tandem Mass Spectrometry (MS/MS): Essays and Tutorials. **2006** (accessed April 16, 2017)
14. Addie, R.D; Balluff, B; Morreau, H; McDonell, L.A; Current state and future challenges of mass spectrometry imaging for clinical research. Analytical Chemistry **2015** 87 6426-6433**.**
15. Goto-Inoue, N; Hayasaka, T; Zaima, N; Setou, M. Imaging mass spectrometry for lipidomics. Biochimica et Biophysica Acta. **2011** 1811(11) 961-969.
16. Rubakhin, S.S; Sweedler , J.V; A mass spectrometry primer for mass spectrometry imaging. Methods Mol Biol **2010** 656 21-49.
17. Bjarnholt, N; Li, B; D'Alvise, J; Janfelt, C. Mass spectrometry imaging of plant metabolite – principles and possibilities. Nat. Prod. Rep **2014** 31 818-837
18. Dong, Y; Li, B; Maltisky, S; Rogachev, I; Aharoni, A; Kaftan, F. Sample preparation for Mass Spectrometry Imaging of Plant Tissues: A Review. Frontiers in Plant Science. **2016** 7(60).

10. ACRONYMS

MALDI	Matrix assisted laser desorption ionization
TOF	Time of flight
LC	Liquid chromatography
GC	Gas chromatography
NMR	Nuclear magnetic resonance
MS	Mass spectrometry
MSI	Mass spectrometry imaging
DHB	2,5-Dihydroxydbenzoic acid
DAN	1,5-Diaminonaphtalene
SA	Sinapinic acid
CHCA	α-cyano-4-hydroxycinnamic acid
ACN	Acetonitrile
TFA	Trifluoracetic acid
ITO	Indium tin oxide
CPF	Chlorpyrifos

APPENDICES

APPENDIX 1: LIPID FRAGMENTATION EXPANSION TABLES

SPHINGOLIPIDS

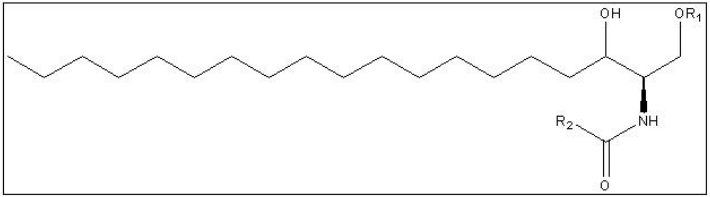

		R2															
		16:0	16:1	16:2	16:3	18:0	18:1	18:2	18:3	20:0	20:1	20:2	20:3	22:0	22:1	22:2	22:3
	R2 chain mass+CO	240	238	236	234	268	266	264	262	296	294	292	290	324	322	320	318
Sphingolipid -CH2OR1	Sphinganine	539	537	535	533	567	565	563	561	595	593	591	589	623	621	619	617
	Sphingosine	537	535	533	531	565	563	561	559	593	591	589	587	621	619	617	615
	Phytoceramide	555	553	551	549	583	581	579	577	611	609	607	605	639	637	635	633

Sphingoid chain

	C18			C18 (-NH)		
R1	Sphinganine	Sphingosine	Phytoceramide	Sphinganine	Sphingosine	Phytoceramide
Sphingomyelin	466	483	500	451	449	469
Ceramide	300	317	334	285	283	303
Glucosylceramide	462	479	496	447	445	465
Sulfatide	526	543	560	511	509	529

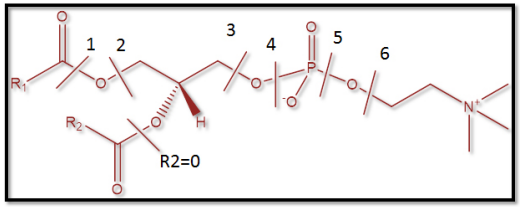

PHOSPHOLIPIDS				R1																	
				C16				C18				C20				C22					
	M-H	No. frag.		16:0	16:1	16:2	16:3	18:0	18:1	18:2	18:3	20:0	20:1	20:2	18:3	22:0	22:1	22:2	20:3		
		1	R1CO	240	238	236	234	268	266	264	262	296	294	292	290	324	322	320	318		
		2	R1COO	255	253	251	249	283	281	279	277	311	309	307	305	339	337	335	333		
R2	0	3	R1COO-CH2COHCH2	312	310	308	306	340	338	336	334	368	366	364	362	396	394	392	390		
		4	R1COO-CH2COHCH2O	328	326	324	322	356	354	352	350	384	382	380	378	412	410	408	406		
		5	R1COO-CH2COHCH2O-PO2	391	389	387	385	419	417	415	413	447	445	443	441	475	473	471	469		
		6	R1COO-CH2COHCH2O-PO3	407	405	403	401	435	433	431	429	463	461	459	457	491	489	487	485		
	16:0	3	R1COO-CH2COR2CH2	552	549	547	545	580	578	576	573	608	606	604	602	636	634	632	630		
		4	R1COO-CH2COR2CH2O	567	565	563	561	596	594	591	589	624	622	620	618	652	650	648	646		
		5	R1COO-CH2COR2CH2O-PO2	630	628	626	624	658	656	654	652	687	685	682	680	715	713	711	709		
		6	R1COO-CH2COR2CH2O-PO3	646	644	642	640	674	672	670	668	703	701	698	696	731	729	727	725		
	16:1	3	R1COO-CH2COR2CH2	549	547	545	543	578	576	573	571	606	604	602	600	634	632	630	628		
		4	R1COO-CH2COR2CH2O	565	563	561	559	594	591	589	587	622	620	618	615	650	648	646	644		
		5	R1COO-CH2COR2CH2O-PO2	628	626	624	622	656	654	652	650	685	682	680	678	713	711	709	706		
		6	R1COO-CH2COR2CH2O-PO3	644	642	640	638	672	670	668	666	701	698	696	694	729	727	725	722		
	16:2	3	R1COO-CH2COR2CH2	547	545	543	541	576	573	571	569	604	602	600	597	632	630	628	626		
		4	R1COO-CH2COR2CH2O	563	561	559	557	591	589	587	585	620	618	615	613	648	646	644	642		
		5	R1COO-CH2COR2CH2O-PO2	626	624	622	620	654	652	650	648	682	680	678	676	711	709	706	704		
		6	R1COO-CH2COR2CH2O-PO3	642	640	638	636	670	668	666	664	698	696	694	692	727	725	722	720		
	16:3	3	R1COO-CH2COR2CH2	545	543	541	539	573	571	569	567	602	600	597	595	630	628	626	624		
		4	R1COO-CH2COR2CH2O	561	559	557	555	589	587	585	583	618	615	613	611	646	644	642	639		
		5	R1COO-CH2COR2CH2O-PO2	624	622	620	618	652	650	648	646	680	678	676	674	709	706	704	702		
		6	R1COO-CH2COR2CH2O-PO3	640	638	636	634	668	666	664	662	696	694	692	690	725	722	720	718		
	18:0	3	R1COO-CH2COR2CH2	580	578	576	573	608	606	604	602	636	634	632	630	664	662	660	658		
		4	R1COO-CH2COR2CH2O	596	594	591	589	624	622	620	618	652	650	648	646	680	678	676	674		
		5	R1COO-CH2COR2CH2O-PO2	658	656	654	652	687	685	682	680	715	713	711	709	743	741	739	737		
		6	R1COO-CH2COR2CH2O-PO3	674	672	670	668	703	701	698	696	731	729	727	725	759	757	755	753		
	18:1	3	R1COO-CH2COR2CH2	578	576	573	571	606	604	602	600	634	632	630	628	662	660	658	656		
		4	R1COO-CH2COR2CH2O	594	591	589	587	622	620	618	615	650	648	646	644	678	676	674	672		
		5	R1COO-CH2COR2CH2O-PO2	656	654	652	650	685	682	680	678	713	711	709	706	741	739	737	735		
		6	R1COO-CH2COR2CH2O-PO3	672	670	668	666	701	698	696	694	729	727	725	722	757	755	753	751		
	18:2	3	R1COO-CH2COR2CH2	576	573	571	569	604	602	600	597	632	630	628	626	660	658	656	654		
		4	R1COO-CH2COR2CH2O	591	589	587	585	620	618	615	613	648	646	644	642	676	674	672	670		
		5	R1COO-CH2COR2CH2O-PO2	654	652	650	648	682	680	678	676	711	709	706	704	739	737	735	733		
		6	R1COO-CH2COR2CH2O-PO3	670	668	666	664	698	696	694	692	727	725	722	720	755	753	751	749		
	18:3	3	R1COO-CH2COR2CH2	573	571	569	567	602	600	597	595	630	628	626	624	658	656	654	652		
		4	R1COO-CH2COR2CH2O	589	587	585	583	618	615	613	611	646	644	642	639	674	672	670	668		
		5	R1COO-CH2COR2CH2O-PO2	652	650	648	646	680	678	676	674	709	706	704	702	737	735	733	730		
		6	R1COO-CH2COR2CH2O-PO3	668	666	664	662	696	694	692	690	725	722	720	718	753	751	749	746		

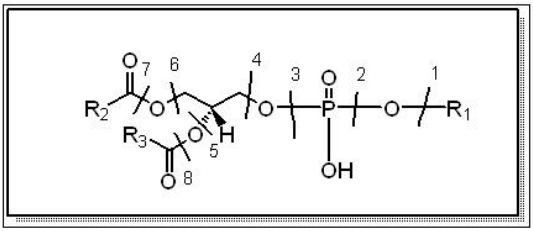

Polar heads

	PA	PE	PC	PG	PS
fragment	H	$(CH_2)_2NH_2$	$(CH_2)_2N(CH_3)_3$	$(CH_2)_3(OH)_2$	$CH_2CHNH_3COO^-$
1	-	45	87.1	75	88
2	17	61	103.1	91	104
3	79.97	124	166.06	154	167
4	95.96	140	182.06	170	183
5+5	123	167	209.08	197	210
5+6	137	181	223.1	211	224
5+7 (8+6)	153	198	239.09	227	240
8+5	139	183	225.08	213	226
8+7	169	213	255.09	243	256

Considering different chain lengths

			PA	PE	PC	PG	PS
R2(+CO)	chain m/z	fragment	H	$(CH_2)_2NH_2$	$(CH_2)_2N(CH_3)_3$	$(CH_2)_3(OH)_2$	$CH_2CHNH_3COO^-$
16:0	240	5	393	438	479	467	480
		8	409	453	495	483	496
16:1	238	5	391	436	477	465	478
		8	407	451	493	481	494
16:2	236	5	389	434	475	463	476
		8	405	449	491	479	492
18:0	268	5	421	466	507	495	508
		8	437	481	523	511	524
18:1	266	5	419	464	505	493	506
		8	435	479	521	509	522
18:2	264	5	417	462	503	491	504
		8	433	477	519	507	520
18:3	262	5	415	460	501	489	502
		8	431	475	517	505	518
20:0	296	5	449	494	535	523	536
		8	465	509	551	539	552
20:1	294	5	447	492	533	521	534
		8	463	507	549	537	550
20:2	292	5	445	490	531	519	532
		8	461	505	547	535	548
20:3	290	5	443	488	529	517	530
		8	459	503	545	533	546
22:0	324	5	477	522	563	551	564
		8	493	537	579	567	580

GALACTOLÍPIDS

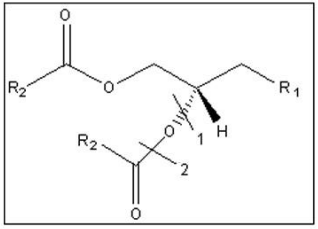

			R2															
			C16 (+CO)				C18(+CO)				C20(+CO)				C22(+CO)			
	R1	Fragment	16:0	16:1	16:2	16:3	18:0	18:1	18:2	18:3	20:0	20:1	20:2	20:3	22:0	22:1	22:2	22:3
MGDG	O-Galactose (179)	1	492	490	488	486	520	518	516	514	548	546	544	542	576	574	572	570
		2	476	474	472	470	504	502	500	498	532	530	528	526	560	558	556	554
DGDG	O-Digalactose (341)	1	654	652	650	648	682	680	678	676	710	708	706	704	738	736	734	732
		2	638	636	634	632	666	664	662	660	694	692	690	688	722	720	718	716
SQDG	O-Sulfoquinovose (243)	1	556	554	552	550	584	582	580	578	612	610	608	606	640	638	636	634
		2	540	538	536	534	568	566	564	562	596	594	592	590	624	622	620	618
			Adduct with Na															
MGDG	O-Galactose (179)	1	515	513	511	509	543	541	539	537	571	569	567	565	599	597	595	593
		2	499	497	495	493	527	525	523	521	555	553	551	549	583	581	579	577
DGDG	O-Digalactose (341)	1	677	675	673	671	705	703	701	699	733	731	729	727	761	759	757	755
		2	661	659	657	655	689	687	685	683	717	715	713	711	745	743	741	739
SQDG	O-Sulfoquinovose (243)	1	579	577	575	573	607	605	603	601	635	633	631	629	663	661	659	657
		2	563	561	559	557	591	589	587	585	619	617	615	613	647	645	643	641